Journal of Applied Fluid Mechanics, Vol. 10, No. 3, pp. 801-811, 2017.
Available online at www.jafmonline.net, ISSN 1735-3572, EISSN 1735-3645.
DOI: 10.18869/acadpub.jafm.73.240.26830

Experimental and Numerical Investigation on Laminar Pipe Flow of Magneto-Rheological Fluids under Applied External Magnetic Field

E. Gedik

Faculty of Technology, Karabük University, Karabük, TR-78050, Turkey

Email: egedik@karabuk.edu.tr

(Received June 27, 2016; accepted January 29, 2017)

ABSTRACT

An experimental and numerical study of Magnetorheological (MR) fluids flow in circular pipes under the influence of uniform magnetic field is considered. In the experiments, an electromagnetic device was manufactured to generate the magnetic field. The experiments were performed using magnetic fields B= 0, 0.01, 0.02, 0.03, 0.04, 0.05, 0.06, 0.07, 0.08, 0.09, 0.1, 0.12 and 0.15 T. Numerical study was performed to show the accuracy of the results obtained from experimental study. In numerical study, Computational Fluid Dynamics (CFD) analysis was used. The ANSYS Fluent 14.0 code based on the finite volume method was used for the CFD analysis. In the experiments, the applied magnetic field decreased the flow rate of the fluids by increasing viscosity. In case of 10 mm pipe diameter, the flow velocity of the A, B and C fluids were obtained as 0.593, 0.749 and 0.938 m/s respectively in situation B=0 T. When magnetic field was applied as B=0.15 T, decreases have occurred in the velocity of A, B and C fluids as 95.27%, 90.24% and 85.6% respectively. Similarly, in case of 15 mm pipe diameter, 96.87%, 95.06% and 90.76% decreases have occurred in the flow velocity of A, B and C fluids having 0.301, 0.363 and 0.445 m/s flow velocity respectively. The results were compared for the magnetic field values B=0, 0.05, 0.10 and 0.15 T. It was found that the differences between experimental and numerical study were found as 6.10% and 1.71% for the B=0 T and B≠0 T situations respectively when the pipe has 10 mm pipe diameter. In case of 15 mm pipe diameter, the differences were found as 2.31% and 0.89%. As a result, it was found that the results obtained from experimental and numerical study were qualitatively and quantitatively in good agreement.

Keywords: Magnetorheological (MR) fluid; Magnetic field; Laminar pipe flow; CFD.

NOMENCLATURE

B	magnetic field intensity	r	radial coordinate
d	pipe diameter	γ	shear rate
dP	pressure drop	z	axial coordinate
L	pipe length		
MR	magnetorheological	ΔP	pressure difference
Q	volumetric flow rate	θ	tangential coordinate
R	pipe radius	u	velocity
Re	Reynolds number	μ	viscosity
		τ	yield stress

1. INTRODUCTION

Flow rate and velocities of some fluids are changed with the effect of magnetic field that depends on magnetization features of materials. Magneto-Rheological (MR) fluids are those which show these features. MR fluids are suspensions of granular particles in a carrier liquid such as water, mineral oil and hydrocarbon based oils (Çeşmeci and Engin 2010; Resiga *et al*. 2010). Particle diameter of these suspensions changes between 1-5 μm. These fluids which have constant viscosity like an ordinary Newtonian fluid show Non-Newtonian flow behaviors when magnetic field is applied to the fluid that causing viscosity to increase. So the viscosity of the MR fluid can be controlled depending on the

applied magnetic field intensity. When the fluid is exposed to the magnetic field the particles are guided by the magnetic field to form a chainlike structure and it becomes semi-solid state. The field-induced transition of these smart fluids from the liquid to a semi-solid state is fast and reversible (Engin *et al*. 2005). This chain-like structure restricts the motion of the fluid and therefore changes the rheological behavior of the fluid (Carlson *et al*. 1995; He and Huang 2005; Olabi and Grunwald 2007; Grunwald and Olabi 2008). The field-dependent rheological changes in MR fluids are primarily observed as a significant increase in the yield shear stress of the fluids, which can be continuously controlled by the intensity of applied magnetic field (Gedik *et al*. 2012). MR fluid technology has been used in various engineering applications. MR dampers used in vibration damping control applications (Weiss *et al*. 1998; Ginder *et al*. 1996; Spencer *et al*. 1997; Dyke *et al*. 1998; Guo and Hu 2005; Boada *et al*. 2011) are devices that work with MR Fluids and recently they are widely used in variety of fields such as automotive industry, military and agricultural trucks (Olabi and Grunwald 2007; Lindler *et al* 2000; Chooi and Oyadiji 2008; Ha *et al* 2009; Hiemenz *et al*. 2009). It has also been widely used for the clutch, brake and locking systems in the automotive sector (Li and Du 2005; Park *et al* 2006; Senkal and Gürocak 2010; 19-21). Similarly, the MR fluids have been used in different areas of industry, structural control applications; for the protection of buildings against earthquake while absorbing vibrations of bridges and buildings during the earthquakes and also absorbing vibrations of washing machines (Carlson and Spencer 1996; Dyke *et al* 1996; Dyke *et al* 1997; Gordaninejad *et al*. 1999; Fujitani *et al*. 2002; Yang *et al*. 2011), to medical area; for the use of prosthetic legs to facilitate the movement (Hsu *et al*. 2006; Jonsdottir *et al*. 2009; Hreinsson 2011) and surface polishing technology (Yan *et al*. 2007; Jha and Jain 2009; Jang *et al*. 2010). Also it will be possible to make robots that can be able to use hands and arms as naturally as people by using MR fluids planned to be used in spacecrafts (Pettersson *et al*. 2010). There are many papers published which deal with the applications of MR fluids and their using specification in the literature. Applied modes of these fluids and rheological properties were detailed by (Costa and Branco 2009; Gedik et al. 2012). Channel and micro-channel flows of MR fluids have been studied by several authors (Bruno et al. 2009; Nishiyama et al. 2011). Flows of MR fluids through different types of porous media have been considered, both theoretically and experimentally by Kuzhir *et al*. 2003. Engin *et al*. 2005 have investigated fully developed laminar flows of water-based MR fluids in micro tubes at various Reynolds and Hedsrom numbers numerically. Bingham plastic model has been used for the MR fluid flow behavior in the study. Kuzhir *et al*. 2009 have investigated axisymmetric flow of a MR fluid through an orifice experimentally and the effect of an external magnetic field, transverse to the flow, was also examined in their paper. Jang *et al*. 2009 have proposed in their study a new model to predict the behavior of MR fluid under arbitrary 3D magnetic and shear strain fields using Lekner summation method. Viscosity testing of MR fluid for different magnetic fields was studied by Roszkowski *et al* 2008. Bica *et al*. 2013 have reviewed the potential applications of magnetorheological suspensions with their rheological and electro-conductive properties under an applied magnetic field. Pressure driven laminar pipe flows of a magnetic fluid in pipes have been studied by Cunha and Sobral 2005. The problem was reduced to a weakly nonlinear ordinary differential equation for the velocity. Friction factor and the velocity profile were presented as a function of magnetic and hydrodynamic physical parameters in the study. Pressure-driven flow under magnetic field has also been investigated by Ramos *et al*. 2005. In the study, a computer simulation based on finite volume method was used to simulate coupled momentum and magnetic equations of a laminar magnetic fluid flow.

In this paper, laminar flow of incompressible MR fluids through cylindrical pipes that have 10 and 15 mm pipe diameter in the presence of a uniform magnetic field applied perpendicularly to the flow direction is carried out. The flow behaviors of three kinds of MR fluids under magnetic field are investigated both experimentally and numerically. An experimental apparatus has been designed and setup to produce electromagnetic field. Experiments are carried out for three MR fluids flow through two cylindrical pipe. Numerical study was performed to show the accuracy of the results obtained from experimental study. In numerical study, Computational Fluid Dynamics (CFD) analysis was used. At the end of the study, experimental and numerical studies were compared with each other and a good agreement has been seen.

2. METHODOLOGY

In this study, pressure-driven laminar flow of viscous incompressible MR fluids that have different physical properties were investigated experimentally and numerically. In the experimental study, to produce magnetic field induction an electromagnetic device has been designed and manufactured. Effect of magnetic field to the laminar flow of fluids in pipes that have 10 and 15 mm inner pipe diameter and 300 mm length is observed. Experiments were performed for the magnetic field induction values of B= 0, 0.01, 0.02, 0.03, 0.04, 0.05, 0.06, 0.07, 0.08, 0.09, 0.10, 0.12 and 0.15 T. To show the accuracy of the results obtained from experimental study a Computational Fluid Dynamics analysis was performed. The equations governing the steady flow of an incompressible MR fluid are implemented in the commercial code ANSYS 14.0 Fluent which is a flexible CFD code based on finite volume approach. Under the normal state MR fluids behave like an ordinary Newtonian fluid unless they are exposed to any magnetic field effect. When they are positioned under any magnetic field induction their viscosity increases as can be seen in Fig.1. For a simple Poiseuille flow in a pipe, the viscosity is expressed as:

$$\mu = \frac{\pi \Delta P R^4}{8LQ} \tag{2.1}$$

where μ (Pas) is the dynamic viscosity of fluids, ΔP (Pa), R (m), L (m) and Q (m^3/s) are the pressure drop, pipe radius, pipe length and the volumetric flow rate respectively. Depending on increasing magnetic field values applied externally perpendicular to the flow direction, viscosity values have been increased. In the numerical simulations these increased viscosity values were used for each magnetic field values.

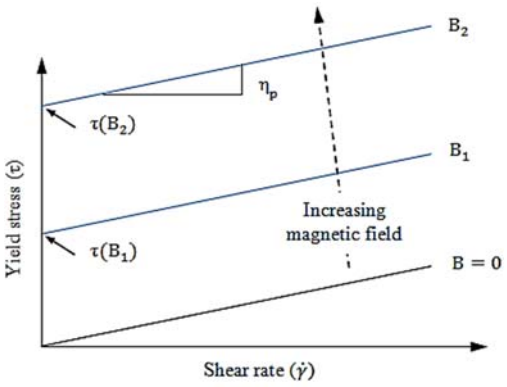

Fig. 1. Behavior of an idealized, Bingham model, MR fluid in the presence of an applied magnetic field (B) as a function of shear rate.

2.1 Experimental Procedure

In this study, the MR fluids of BASONETIC 5030-4035-2040 were used developed by BASF CO.LTD. GERMANY. The densities are 4.12, 2.68, 2.47 g/cm^3 respectively at room temperature. BASONETIC 5030, 4035 and 2040 have 47%, 26.6% and 24% volumetric concentration of carbonyl iron powder respectively. We prepared 20%, 15% and 10% of these MR fluid samples by diluting base fluid, poly-α-olefin and called them A, B and C fluids respectively. These prepared fluids were used in all the experiments and numerical studies whose physical properties are given in Table 1. To determine the viscosity of the MR fluids MALVERN/BOHLIN GEMINI 2 MODEL rheometer was used. As a result of the viscosity measurements 0.909, 0.710 and 0.454 Pas values were measured for fluids A, B and C at 40 °C and γ=99.55 1/s shear rate without applied magnetic field intensity.

Table 1 Physical properties of the fluids

	A	B	C
Density (g/cm^3)	1.8	1.5	1.3
Viscosity (Pas, measured at 40 °C, γ=99.55 1/s)	0.909	0.710	0.454
Concentration (%)	20	15	10
Base Fluid	Poly-α-olefin		
Magnetizable particle	Carbonyl Iron Powder		
Temperature range (°C)	-40 °C to + 120 °C		

An experimental rig was established to study the laminar flow of MR fluids past circular pipes in the presence of an external magnetic field as shown schematically in Fig. 2. The experimental system mainly includes a pump, a flow test section, electromagnet, computer, and a reservoir and fluid collection tank. In the test section, pressure transmitters in which pressure measurement ranges between ±100 and ±500 mbar with ± 0.01 accuracy were used to measure the pressure difference between inlet and outlet of the pipes positioned inside the magnetic field.

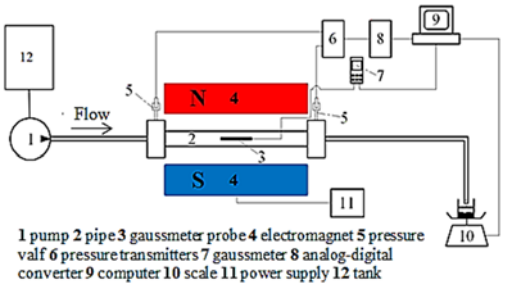

Fig. 2. Schematic illustration of the experimental apparatus (Gedik, 2012).

Applied magnetic field values were also measured in this section via F.W.BELL 5180 Gauss/Tesla Meter that can be able to do 0-3 T measurement with ±0.01 accuracy and is connectable to computer by USB connection. Mass flow rate measurements were made by using KERN PLE 3100-2N model digital scale that has maximum 3100 g and minimum 50 mg measurement capacity with ± 0.02 g measurement accuracy. To generate the magnetic field across the gap in the electromagnetic device, a current supply powered by a 220 V AC power supply was used. An experimental apparatus has been shown in Fig.3.

Fig. 3. Experimental apparatus.

In this figure, fluid that filled reservoir tank (12) is circulated by the pump (1) to the pipe (2) that is positioned between the electromagnetic poles (4) and then it is collected in the collection tank standing on

precision scale (10). Connecting the pressure transmitters (6) to the inlet and outlet sections of the pipe positioned inside the magnetic field, pressure values are recorded to the computer (9) via analog-digital converter (8). Similarly, measuring magnetic fields' values via Gaussmeter (7) probe (3) positioned between N-S poles of the electromagnetic device, they are recorded to the computer. In addition, the mass flow rate of fluids collected in the collection tank standing on precision scale is recorded to computer. All measuring data is carried out by a software program during the experiments. Current, which must be given to the electromagnetic coils to create the desired magnetic field values in the electromagnetic device, is supplied by a power supply (11) that is connected to the system.

2.2 Numerical Technique

In this paper, we have also studied numerically, to show the accuracy of the results that are obtained from experimental studies. The fundamental conversation of the mass and momentum equations the steady motion of an incompressible MR fluid under magnetic field in a cylindrical pipe are:

$$\nabla . \mathbf{V} = 0 \tag{2.2}$$

$$\rho \frac{\mathrm{D}\mathbf{V}}{\mathrm{D}t} = -\mathrm{N} + \mu \Delta \mathbf{V} \tag{2.3}$$

where N indicates the pressure gradient ($\partial \mathrm{P}/\partial \mathrm{z}$) (Pa/m), ρ the fluid density (kg/m^3), μ the dynamic viscosity of the fluid (kg/ms). To adding electromagnetic force term, Equation 2.3 can be expressed as:

$$\rho \frac{\mathrm{D}\mathbf{V}}{\mathrm{D}t} = -\mathrm{N} + \mu \Delta \mathbf{V} + \mathbf{F}_{\mathrm{EM}} \tag{2.4}$$

where $\mathbf{F}_{\mathrm{EM}}$ is the electromagnetic force which expressed as follow:

$$\mathbf{F}_{\mathrm{EM}} = \eta(\mathbf{J} \times \mathbf{H}) = \mathbf{J} \times \mathbf{B} \tag{2.5}$$

In Equation 2.5 **J** indicates the electric current intensity which is expressed as below according to the Ohm law:

$$\mathbf{J} = \sigma(\mathbf{E} + \mathbf{V} \times \mathbf{B}) \tag{2.6}$$

Where σ indicates the electrical conductivity of the fluid, **E** magnitude of electrical field, **V** average flow velocity vector and **B** is the magnetic field induction. In order to be able to investigate how fluid will be affected from the magnetic field applied perpendicular the flow, the mathematical model is obtained as follow for the r, θ and z components of the equation of motion.

r – component:

$$\rho\left(\mathrm{v_r}\frac{\partial \mathrm{v_r}}{\partial \mathrm{r}} + \frac{\mathrm{v_\theta}}{\mathrm{r}}\frac{\partial \mathrm{v_r}}{\partial \theta} - \frac{{\mathrm{v_\theta}}^2}{\mathrm{r}} + \mathrm{v_z}\frac{\partial \mathrm{v_r}}{\partial \mathrm{z}}\right) = -\frac{\partial \mathrm{p}}{\partial \mathrm{r}} + \mu\left(\frac{\partial^2 \mathrm{v_r}}{\partial \mathrm{r}^2} + \frac{1}{\mathrm{r}}\frac{\partial \mathrm{v_r}}{\partial \mathrm{r}} - \frac{\mathrm{v_r}}{\mathrm{r}^2} + \frac{1}{\mathrm{r}^2}\frac{\partial^2 \mathrm{v_r}}{\partial \theta^2} - \frac{2}{\mathrm{r}^2}\frac{\partial \mathrm{v_\theta}}{\partial \theta} + \frac{\partial^2 \mathrm{v_r}}{\partial \mathrm{z}^2}\right) + \sigma(\mathrm{E_0} - \mathrm{B_0 v_r})\mathrm{B_0} \tag{2.7}$$

θ - component:

$$\rho\left(\mathrm{v_r}\frac{\partial \mathrm{v_\theta}}{\partial \mathrm{r}} + \frac{\mathrm{v_\theta}}{\mathrm{r}}\frac{\partial \mathrm{v_\theta}}{\partial \theta} - \frac{\mathrm{v_{r1}v_\theta}}{\mathrm{r}} + \mathrm{v_z}\frac{\partial \mathrm{v_\theta}}{\partial \mathrm{z}}\right) = -\frac{1}{\mathrm{r}}\frac{\partial \mathrm{p}}{\partial \theta} + \mu\left(\frac{\partial^2 \mathrm{v_\theta}}{\partial \mathrm{r}^2} + \frac{1}{\mathrm{r}}\frac{\partial \mathrm{v_\theta}}{\partial \mathrm{r}} - \frac{\mathrm{v_\theta}}{\mathrm{r}^2} + \frac{1}{\mathrm{r}^2}\frac{\partial^2 \mathrm{v_\theta}}{\partial \theta^2} + \frac{2}{\mathrm{r}^2}\frac{\partial \mathrm{v_r}}{\partial \theta} + \frac{\partial^2 \mathrm{v_\theta}}{\partial \mathrm{z}^2}\right) + \sigma(\mathrm{E_0} - \mathrm{B_0 v_\theta})\mathrm{B_0} \tag{2.8}$$

z - component:

$$\rho\left(\mathrm{v_r}\frac{\partial \mathrm{v_z}}{\partial \mathrm{r}} + \frac{\mathrm{v_\theta}}{\mathrm{r}}\frac{\partial \mathrm{v_z}}{\partial \theta} + \mathrm{v_z}\frac{\partial \mathrm{v_z}}{\partial \mathrm{z}}\right) = -\frac{\partial \mathrm{p}}{\partial \mathrm{z}} + \mu\left(\frac{\partial^2 \mathrm{v_z}}{\partial \mathrm{r}^2} + \frac{1}{\mathrm{r}}\frac{\partial \mathrm{v_z}}{\partial \mathrm{r}} + \frac{1}{\mathrm{r}^2}\frac{\partial^2 \mathrm{v_z}}{\partial \theta^2} + \frac{\partial^2 \mathrm{v_z}}{\partial \mathrm{z}^2}\right) + \sigma(\mathrm{E_0} - \mathrm{B_0 v_z})\mathrm{B_0} \tag{2.9}$$

Boundary conditions:

$$v_r(r,0) = 0;\ v_\theta(r,0) = 0;\ v_z(r,0) = u \tag{2.10}$$

$$\frac{\partial P}{\partial r} = 0;\ \frac{\partial P}{\partial \theta} = 0;\ \frac{\partial P}{\partial z} = C \tag{2.11}$$

$$E_0 = 0;\ B_0 = B \tag{2.12}$$

The governing equations (Eqs. (2.7)- (2.9)) with the associated boundary conditions (Eqs. 2.10-12) are solved with using Academic version licensed ANSYS Fluent 14.0 code based on finite volume method for the Computational Fluid Dynamics (CFD) analysis. Laminar flows of three kinds of MR fluids in two different pipes are carried out for the CFD analysis. Initially, the flow model geometry was designed and created considering the pipe geometries that are used in the experiments in Gambit 2.3.16 pre-processor and then it was imported to ANSYS Fluent code for the solution of 3D laminar flow as can be seen from the Fig. 4. For the discretization of spatial terms, Green-Gauss cell a second-order upwind scheme is used for the momentum terms of mathematical model, and the SIMPLE Algorithm (Patankar 1980; Mistrangelo 2006) is used to determine the coupled pressure-velocity gradients. The convergence is declared when the maximum relative change between two consecutive iteration levels fell below than 10^{-6}. The wall boundary conditions were implemented as stationary wall and no slip conditions by means of user profile functions.

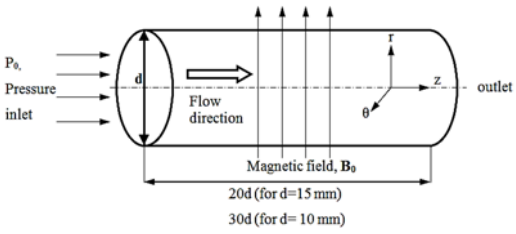

Fig. 4. Schematic view of pipe geometry used in experiments and CFD simulations.

Mesh convergence study was performed for two pipe geometries that have 15 and 10 mm pipe diameters and 300 mm pipe length. Axial velocity distributions are given for the four mesh size values without magnetic field in the Fig. 5.

As can be seen clearly from the figure, the smaller mesh size (increasing mesh density) increased velocities and after a certain mesh size, a significant change was not observed on the velocities. Fine mesh size were determined as 1 mm for the 15 mm pipe while it was 0.5 mm for the pipe that is 10 mm

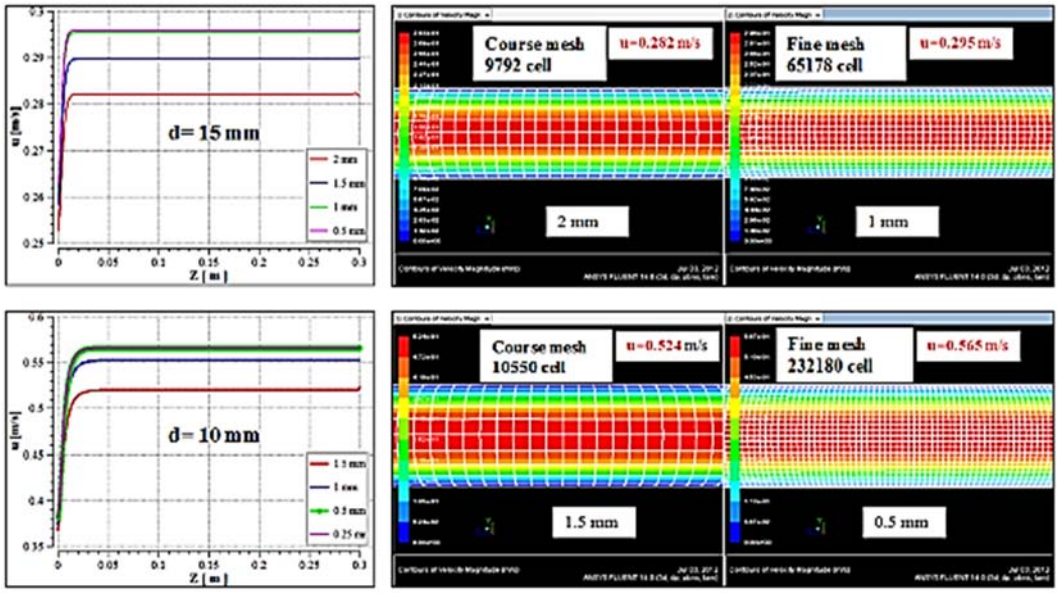

Fig. 5. Mesh convergence study for d=15 and 10 mm.

in diameter. Mesh convergence study information for two pipes' geometries are given in Table.2.

For the solution of problem, 65178 and 232180 hexahedra type elements were used for the 15 and 10 mm pipe diameter respectively. After finding the fine mesh, the creating mesh was imported to FLUENT 14.0 software. The discrete system of linearized equations was solved by an iterative procedure. During CFD simulation procedure, the viscosity values obtained from experimental study were used for every applied magnetic field values, so the same conditions were adjusted both in experimental and numerical studies.

Table 2 Mesh information

Diameter (mm)	Mesh No	Mesh size (mm)	Cell number	Iteration	Velocity (m/s)
15	1a	2.0	9792	114	0.282
	2a	1.5	18156	142	0.289
	3a	1.0	65178	313	0.295
	4a	0.5	484380	700	0.295
10	1b	1.5	10550	130	0.524
	2b	1.0	27234	200	0.556
	3b	0.5	232180	601	0.565
	4b	0.25	1670962	1273	0.565

3. RESULTS AND DISCUSSION

In this paper, the flow of MR fluid in circular pipes under the influence of magnetic field was examined experimentally and numerically. In the experiments, to investigate the effect of the magnetic field to the flow velocities, flow rates and pressure drop; an experimental rig has been designed and established. Experiments were performed using the magnetic fields B= 0, 0.01, 0.02, 0.03, 0.04, 0.05, 0.06, 0.07, 0.08, 0.09, 0.1, 0.12 and 0.15 T, whereas B= 0, 0.05, 0.10 and 0.15 T were used in the numerical study to validation of experimental results. ANSYS Fluent CFD package program was used for the numerical study. Results obtained from experimental and numerical studies were compared with each other and various graphs have been plotted depending on flow velocities, pressure drop, magnetic field intensity, non-dimensional velocity u/u_{max} and Re number. Hereafter, these graphs were discussed in the paper. According to the results obtained from the experimental study, axial velocity profiles of A, B and C fluids have been plotted in Fig.6 for two pipes that have 15 and 10 mm pipe diameter with and without applied magnetic field. As can be seen clearly from the figure, the velocity value becomes 0.301 m/s at B=0 T situation for the fluid A in 15 mm pipe, decreasing depending on the increasing magnetic field intensity. As a result of these decreases, velocity values of the flow were found as 0.253, 0.228, 0.206, 0.182, 0.157, 0.133, 0.125, 0.115, 0.094, 0.079, 0.050 and 0.0094 m/s for the magnetic field, B=0.01, 0.02, 0.03, 0.04, 0.05, 0.06, 0.07, 0.08, 0.09, 0.1, 0.12 and 0.15 T respectively. Similarly, these values turned out to be 0.572, 0.553, 0.524, 0.495, 0.449, 0.399, 0.352, 0.309, 0.247, 0.190, 0.111 and 0.028 m/s at the same increasing B values for the 10 mm pipe diameter while it was 0.593 m/s at B=0 T situation. Same tendency can be seen for the fluids B and C in the graphs. Increasing magnetic field intensity has caused the decrease of flow velocities for all MR fluids and decreasing pipe diameter increases the flow velocity as expected. Pressure differences measured in the experimental study and velocity variations inside the pipe center depend on increasing magnetic field intensity is shown in Fig.7 for the pipe that has 15 mm diameter. As can be seen

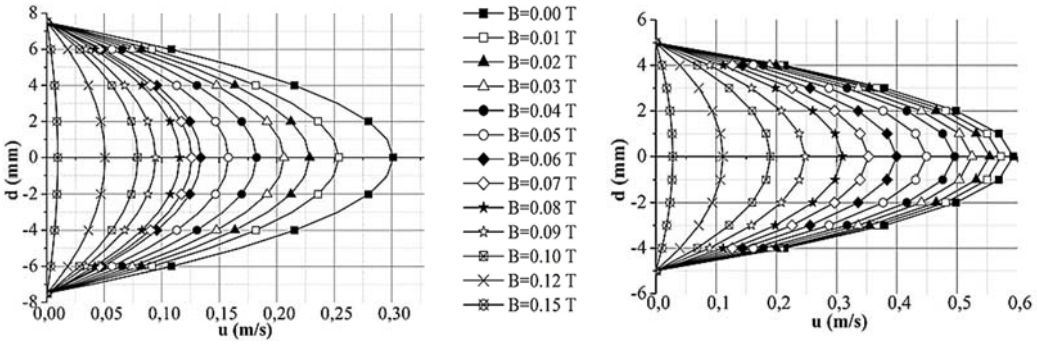

a) fluid A, pipe 15 mm. b) fluid A, pipe 10 mm.

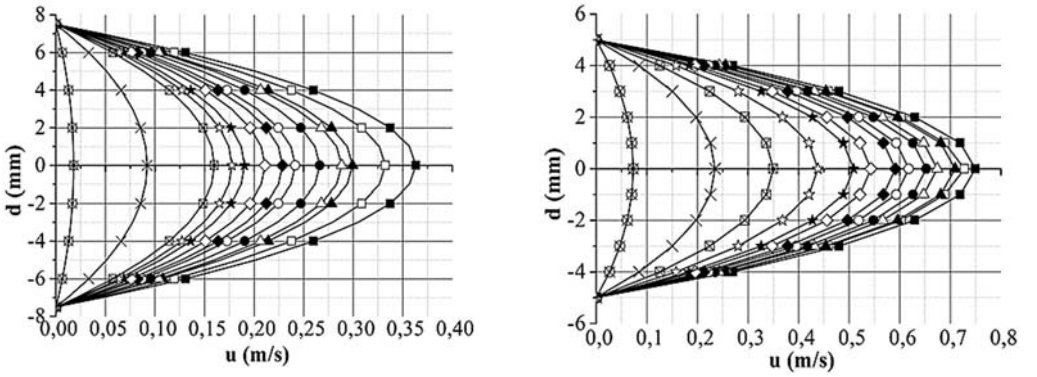

c) fluid B, pipe 15 mm. d) fluid B, pipe 10 mm.

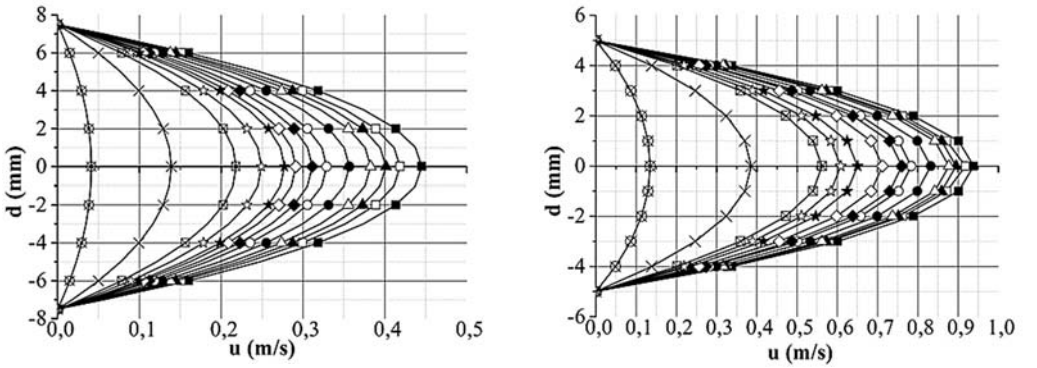

e) fluid C, pipe 15 mm. f) fluid C, pipe 10 mm.

Fig. 6. Variations of experimental velocity profiles depending on increasing magnetic field for A, B, C fluids and d=10 and 15 mm.

clearly from the figure, when the magnetic field increases, velocity values of each of the three fluids decrease whereas pressure values increase. Pressure values that are measured as 5.845, 5.504 and 4.313 kPa in the situation of non-applied magnetic field (B=0T) for the fluids A, B and C respectively, have increased in the presence of magnetic field and these values have become 152.394, 112.610 and 82.147 kPa respectively for the magnetic field value B=0.15 T. In addition, those pressure values have decreased with decreasing densities. In Fig. 8, numerical velocity vectors plotted at $r_{1\text{-}2}$=-0.075-0.075, $\theta_{1\text{-}2}$=0-0, $z_{1\text{-}2}$=0.15-0.15 position of the pipe that has 15 mm diameter are shown for the fluid A. It is clearly seen from the figure the externally applied magnetic field has caused to suppress MR fluid flowing inside the pipe resulted velocity to decrease.

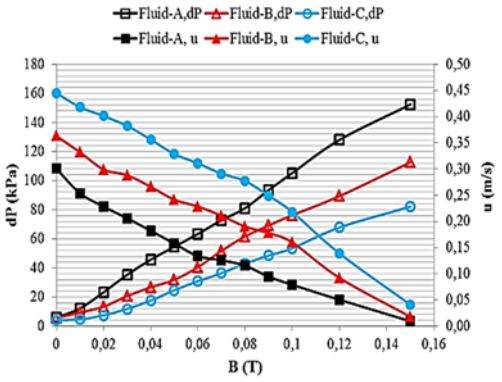

Fig. 7. Variations of pressure and velocities depending on increasing magnetic field intensity for d= 15 mm.

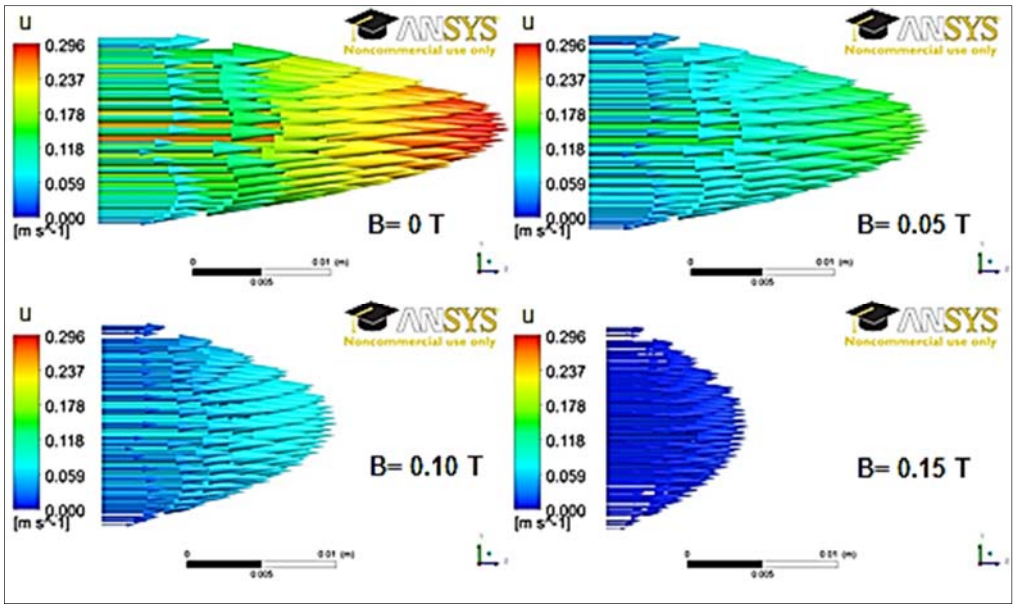

Fig. 8. Numerical velocity vectors under different magnetic field intensities, for d=15 mm, fluid A.

The fluid flow has eventuated at smaller flow rates in B≠0 situations when it is compared to the situation in which there is absence of magnetic field intensity.

When B=0 T, velocity value is computed as 0.295 m/s. The fluid flow has eventuated at smaller flow rates in B≠0 situations when it is compared to the situation in which there is absence of magnetic field intensity. Increasing magnetic field intensity leads to decrease flow velocities and they were computed as 0.155, 0.078 and 0.0093 m/s for the magnetic fields, B=0.05, 0.10 and 0.15 T respectively. At none and low magnetic field values, the axial velocity profile is parabolic and as B increases, the profiles become flattened as can be seen clearly from Fig.8.

Changing of non-dimensional u/u_{max} and Re number values of each of the fluids flow in two pipes has been shown in the Fig. 9. In addition that experimental and numerical results were compared in this figure. Difference of the results that are obtained from experimental and numerical study is found 1.7% in the situation B=0 T, while it was found 1.25%, 1.19% and 1.12% at B=0.05, 0.10 and 0.15 T respectively for the fluid A. It occurred for the B and C fluids as 2.43%, 1.95%, 1.56%, 1.41% and 2.82%, 2.54%, 2.44%, 2.01% at the magnetic fields, B=0, 0.05,0.10, 0.15 T respectively for the pipe that has 15 mm diameter. These differences were computed along pipe diameter and averaged. It is clearly seen from the figure for all the fluids and pipes, that there are very small changes in Re numbers of the fluid under the influence of magnetic field intensity with respect to the fluid under no magnetic field. Maximum Re number has been realized at 0.715 experimental non dimensional velocity value while it was 0.641 numerical non dimensional velocity for all the fluids in pipe that has 15 mm diameter. Reynolds number decreases as the non-dimensional velocity ratio becomes away from this value.

Similarly, the difference of the results that are obtained from experimental and numerical studies is found 4.46% in the situation B=0 T, while it was found 0.80%, 0.74% and 0.63% at B=0.05, 0.10 and 0.15 T respectively for the fluid A. It occurred for the B and C fluids as 6.38%, 0.93%, 0.86%, 0.76% and 7.66%, 1.37%, 1.06%, 0.88% at the magnetic fields, B=0, 0.05,0.10, 0.15 T respectively for the pipe that has 10 mm diameter. Maximum Re number has been realized at 0.640 experimental non dimensional velocity value while it was 0.602 numerical non dimensional velocity for all the fluids in pipe that has 10 mm diameter. Reynolds number decreases as the non-dimensional velocity ratio becomes away from this value. As can be seen from Fig.9 experimental and numerical results are in good agreement with all B, magnetic field values. The maximum difference between experimental and numerical results has been occurred for the C fluid at B=0 T in pipe that has 10 mm diameter. To see these differences clearly Figs 10 and 11 were plotted for the pipes 15 and 10 mm in diameter respectively. Changings of the flow velocities along pipe diameter depending on increasing magnetic field intensity for all the fluids have been plotted in the Figs. 10 and 11.

4. CONCLUSION

In this study, laminar flows of viscous, incompressible three kinds of MR fluids were investigated experimentally and numerically. An experimental rig was designed and established for the experiments. The experiments were performed using the magnetic fields B= 0, 0.01, 0.02, 0.03, 0.04, 0.05, 0.06, 0.07, 0.08, 0.09, 0.10, 0.12 and 0.15 T. A CFD tool was used to study numerically. Results

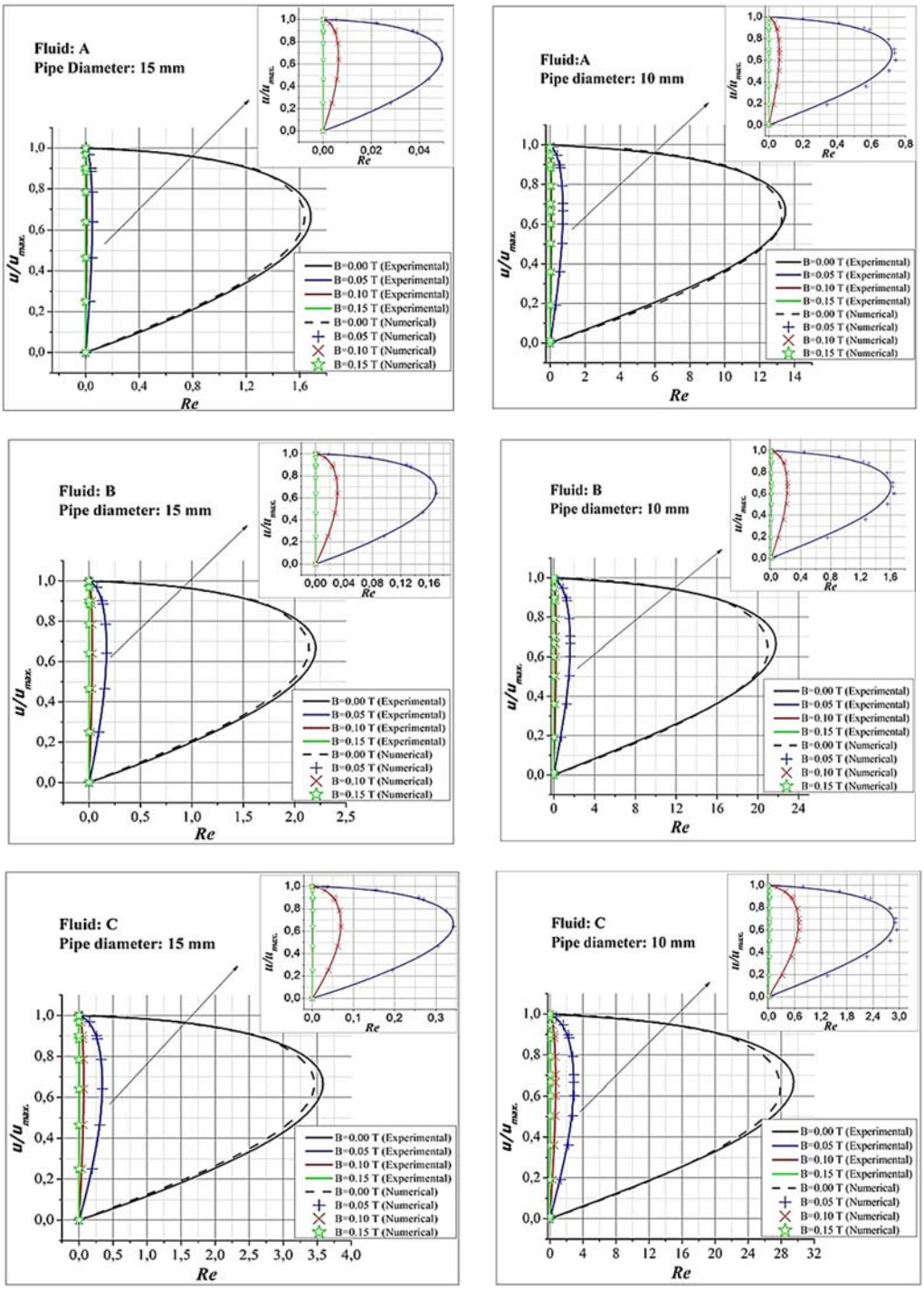

Fig. 9. Experimental and numerical u/u_{max} change versus Re number for d=10 and 15 mm.

obtained from experimental and numerical studies were compared and a good agreement was seen between the two methods. Some following numerical results have been obtained from both studies; In the experiments, axial velocity values have been found as 0.301, 0.363 and 0.445 m/s for the fluid A, B and C respectively for the pipe that has 15 mm diameter, when B=0 T. These values have shown the maximum decrease as 96.87%, 95.06% and 90.76% for the fluids A, B and C respectively, in the situation B=0.15 T where applied magnetic field intensity has the maximum value. In the pipe that has 10 mm diameter, these values have been found as 0.593, 0.749 and 0.938 for the fluids A, B and C respectively when B=0 T. These values have shown the maximum decrease as well, as 95.27%, 90.24% and 85.6% for the fluids A, B and C respectively, in the situation B=0.15 T where applied magnetic field intensity has the maximum value. The results obtained from CFD analysis using B=0, 0.05, 0.1 and

0.15 T were compared with experimental results and it was found that the differences between the experimental and numerical studies were 2.31% and 0.89% for the B=0 and B≠0 T situations respectively for 15 mm pipe diameter, while it was found as 6.10% and 1.71% in case of 10 mm pipe diameter. Consequently;

- ✓ In both studies those are experimental and numerical, the increasing magnetic field that has caused the viscosities of the fluids to increase caused velocities to decrease.
- ✓ Flow velocities and rates have increased with decreased pipe diameter.
- ✓ As the densities of fluids rise, the situation that they were influenced by the magnetic field was more and has caused the more flow reductions.
- ✓ The results obtained from experimental and numerical studies were qualitatively and quantitatively in good agreement.
- ✓ This study will be helpful for the future studies considering MR or magnetic fluids flow and there will be knowledge in the design and produce of some useful devices using MR or magnetic fluids.
- ✓ Next studies can include, more complex flows in pipes or ducts that have different diameters and lengths.

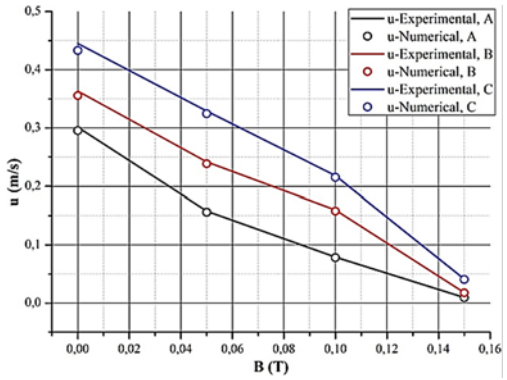

Fig. 10. Experimental and numerical velocity variations depending on increasing magnetic field, at the center of the pipe (d=15 mm).

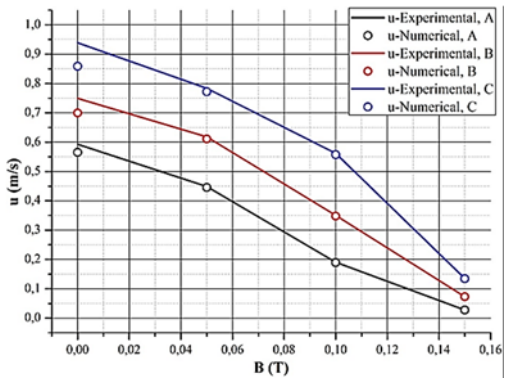

Fig. 11. Experimental and numerical velocity variations depending on increasing magnetic field, at the center of the pipe (d=10 mm).

ACKNOWLEDGEMENTS

The author would like to thank to the Scientific and Technological Research Council of TURKEY (TUBITAK) for providing the financial supports for this study under the 110M030 project.

REFERENCES

Bica, I., Y. D. Liu and H. J Choi (2013). Physical characteristics of magnetorheological suspensions and their applications. Journal of Industrial and Engineering Chemistry 19, 394-406.

Boada, M. J. L, J. A. Calvo, B. L. Boada and V. Díaz (2011). Modeling of a magnetorheological damper by recursive lazy learning. International Journal of Non-Linear Mechanics 46, 479-485.

Bruno, N. M., C. Ciocanel and A. Kipple (2009). Modeling flow of Magnetorheological Fluid through a Micro-channel. *Excerpt from the Proceedings of the COMSOL Conference*, Boston.

Carlson, J. D. and B. F. Spencer (1996). Magneto rheological Fluid dampers for semi-active seismic control. *In the proceeding of the 3rd International Conference Motion and Vibration Control, Chiba-Japan,* 35-40.

Carlson, J. D., D. M. Catanzarite and K. A. Clair (1995 July). Commercial magneto-rheological fluid devices. *In: 5th International conference on electro-rheological, magneto-rheological suspension and associated tech*, Sheffield.

Çeşmeci, Ş. and T. Engin (2010). Modeling and testing of a field-controllable magnetorheological fluid damper. International Journal of Mechanical Science 52, 1036-1046.

Chooi, W.W and S. O. Oyadiji (2008). Design, modelling and testing of magnetorheological (MR) dampers using analytical flow solutions. Computer & and Structures 86, 473-482.

Costa, E and P. J. C. Branco (2009). Continuum electromechanics of a magnetorheological damper including the friction force effects between the MR fluid and device walls: Analytical modeling and experimental validation. Sensors and Actuators A 155, 82-88.

Cunha, F. R and Y. D. Sobral (2005). Asymptotic solution for pressure-driven flows of magnetic fluids in pipes. Journal of Magnetism and Magnetic Materials 289, 314-317.

Dyke, S. J., B. F. Spencer, M. K. Sain and J. D. Carlson (1998). An experimental study of MR dampers for seismic protection. Journal of Smart Materials and Structures: Special Issue on Large Civil Structure 7, 693-703.

Dyke, S. J., B. F. Spencer, M. K. Sain and J. D. Carlson (1996). Modelling and control of magnetorheological fluid dampers for seismic response reduction, Smart Material and

Structure 5, 565-575.

Dyke, S. J., B. F. Spencer, M. K. Sain and J. D. Carlson (1997). On the efficacy of magnetorheological dampers for seismic response reduction. *Proceed ASME Biennial Conference on Vibration and Noise, Sacramento-California.*

Engin, T. C. E. and F. Gordaninejad (2005). Numerical simulation of laminar flow of water-based magneto-rheological fluids in micro tubes with wall roughness effect. International Communication Heat and Mass Transfer 32, 1016-25.

Fujitani, H., Y. Shiozaki, T. Hiwatashi, K. Hata, T. Tomura, H. Sodeyama and S. Soda (2002). A research and development of smart building structures by magneto-rheological damper. Advanced in Building Technologies 1, 473-480.

Gedik, E. (2012). Experimental investigation of magnetohydrodynamic flow in cıcrcular pipes and numerical analysis wıth computational fluid dynamics. Ph. D. thesis, University of Karabük, Turkey.

Gedik, E. H. Kurt, Z. Recebli and C. Balan (2012). Two-dimensional CFD simulation of magnetorheological fluid between two fixed parallel plates applied external magnetic field. Computers and Fluids 63, 128-134.

Ginder, J. M., L. C. Davis and L. D. Elie (1996). Rheology of Magnetorheological Fluids: Models and Measurements. International Journal of Modern Physics B 10, 3293-3303.

Gordaninejad, F. M. Saiidi, B. C. Hansen and F. K. Chang (1999). Magnetorheological fluids dampers for control of bridges. *Proceedings of the Second World Conference on Structure Control Kyoto-Japan*, 991-1000.

Grunwald, A. and A. G. Olabi (2008). Design of magneto-rheological (MR) valve. Sensors Actuators A 148, 211-223.

Guo, D. and H. Hu (2005). Nonlinear Stiffness of a Magneto-Rheological Damper. Nonlinear Dynamic. 40, 241-249.

Ha, S. H., S. B. Choi, E. J. Rhee and P. S. Kang (2009). Optimal design of a magnetorheological fluid suspension for tracked vehicle. *Journal of Physics: Conf Series* 149, 012053

He, J. M.0 and J. Huang (2005). Magnetorheological fluids and their properties. International Journal of Modern Physics B 19, 593-596.

Hieme nz, G. J., W. Hu and N. M. Wereley (2009). Adaptive Magnetorheological seat suspension for the expeditionary fighting vehicle. *Journal of Physics: Conf Series* 149, 012054.

Hreinsson, E. (2011). Durability of a magnetorheological fluid in a prosthetic knee joint. Ph. D. thesis, University of Iceland.

Hsu, H. C. R. Bisbee, M. L. Palmer, R. J. Lukasiewicz, M. W. Lindsay and S. W. Prince (2006). Magnetorheological fluid compositions and prosthetic knees utilizing same. Patent 7101487 ABD.

Jang, K. I., J. Seok, B. K. Min and S. J. Lee (2009). Behavioral model for magnetorheological fluid under a magnetic field using Lekner summation method. Journal of Magnetism and Magnetic Materials 321, 1167-1176.

Jang, K. I., J. Seok, B. K. Min and S. J. Lee (2010). An electrochemomechanical polishing process using magnetorheological fluid. International Journal of Machine Tools & Manufacture 50, 869-881.

Jha, S. and V. K. Jain (2009). Rheological characterization of magnetorheological polishing fluid for MRAFF. The International Journal of Advanced Manufacturing Technology 42, 656-668.

Jonsdottir, F., E. T. Thorarinsson, H. Palsson and K. H. Gudmundsson (2009). Influence of parameter variations on the braking torque of a magnetorheological prosthetic knee. Journal of Intelligent Materials Systems and Structures 20, 659-667.

Kuzhir, P., G. Bossis, V. Bashtovoi and O. Volkova (2003). Flow of magnetorheological fluid through porous media. European Journal of Mechanics-B/Fluids 22, 331-343.

Kuzhir, P., M. T. Lopez and G. Bossis (2009). Abrupt contraction flow of magnetorheological fluids. Physics of Fluids 21, 053101.

Li, W. H. and H. Du (2003). Design and experimental evaluation of a magnetorheological brake. The International Journal of Advanced Manufacturing Technology 21, 508-515.

Lindler, J. E, G. A. Dimock and N. M. Wereley (2000). Design of a magnetorheological automotive shock absorber. *Proceedings SPIE* 1, 426-437.

Mistrangelo, C. (2006). Three-Dimensional MHD flow in sudden expansions. Ph. D. thesis, Institut für Kern-und Energietechnik, Karlsruhe, Germany.

Nishiyama, H., H. Takana, K. Shinohara, K. Mizuki, K. Katagiri and M. Ohta (2011). Experimental analysis on MR fluid channel flow Dynamics with complex fluid-wall interactions. Journal of Magnetism and Magnetic Materials 323, 1293-1297.

Olabi, A. G. and A. Grunwald (2007). Design and application of magneto-rheological fluid. Materials Design 28, 2658-2664.

Park, E. J., D. Stoikov, L. F. Luz and A. Suleman (2006). A performance evaluation of an automotive magnetorheological brake design with a sliding mode controller. Mechatronics 16, 405-416.

Patankar, S. (1980). Numerical heat transfer and fluid flow. Hemisphere Publ. Co., Washington.

Pettersson, A., S. Davis, J. O. Gray, T. J. Dodd and T. Ohlsson (2010). Design of a magnetorheological robot gripper for handling of delicate food products with varying shapes Journal of Food Engineering 98, 332-338.

Ramos, D. M., F. R. Cunha, Y. D. Sobral and J. L. A. F. Rodrigues (2005). Computer simulations of magnetic fluids in laminar pipe flows. Journal of Magnetism and Magnetic Materials 289, 238-241.

Resiga, D. S., D. Bica and L. Vekas (2010). Flow behavior of extremely bidisperse magnetizable fluids. Journal of Magnetism and Magnetic Materials 322, 166-3172.

Roszkowski, A., M. Bogdan, W. Skoczynski and B. Marek (2008). Testing viscosity of MR Fluid in magnetic field, Measurement Science Reviews 8, 5-60.

Şenkal, D. and H. Gurocak (2010). Serpentine flux path for high torque MRF brakes in haptics applications. Mechatronics 20, 377-383.

Spencer, B. F., S. J. Dyke, M. K. Sain and J. D. Carlson (1997). Phenomenological Model for Magnetorheological Dampers. Journal of Engineering Mechanics 123, 230-238.

Weiss, K. D., J. D. Carlson and D. A. Nixon (1994). Viscoelastic Properties of Magneto and Electro Rheological Fluids. Journal of Intelligent Material System and Structure 5, 772-775.

Yan, Y., K. Boseon, H. Shiguo and C. Xing (2007). Glass polishing technology using MR fluids. Journal of Rare Earths 25, 367-369.

Yang, M. G., Z. Q. Chen and X. G. Hua (2011). An experimental study on using MR damper to mitigate longitudinal seismic response of a suspension bridge. Soil Dynamic and Earthquake Engineering 31, 1171-1181.